Building and Environment 80 (2014) 1–10

Contents lists available at ScienceDirect

Building and Environment

journal homepage: www.elsevier.com/locate/buildenv

Numerical and experimental study of a HVAC wall diffuser

J.J. Martinez-Almansa [a, b], A. Fernandez-Gutierrez [c], L. Parras [a, b, *], C. del Pino [b]

[a] ONE GO TECHNOLOGIES S.L, Avda. Cantarrana 13 1 B, 27850 Viveiro, Lugo, Spain
[b] Universidad de Málaga, E.T.S. Ingenieros Industriales, 29071 Málaga, Spain
[c] Universidad de Málaga, Departamento de Máquinas y Motores Térmicos, 29071 Málaga, Spain

ARTICLE INFO

Article history:
Received 23 December 2013
Received in revised form
13 April 2014
Accepted 2 May 2014
Available online 27 May 2014

Keywords:
HVAC
Air
Diffuser
CFD
MMLA

ABSTRACT

In this paper we have developed a Micro/Macro Level Approach (MMLA) method to model a conventional diffuser. This procedure reduces the number of points in order to solve the airflow in a room. This can be seen as a numerical box method, and it provides a number of variables at the inlet of the room (outlet of the diffuser) which are difficult to obtain experimentally, e.g. turbulent properties. Flow visualizations have been carried out to determine the shape of the plume. These qualitative experimental data are also compared with numerical temperature fields for sufficiently high Reynolds numbers and give accurate results. In addition, we report the throw and drop of the diffuser for different flow rates. Finally, the pressure drop of the terminal device has been obtained experimentally, and it is also shown that numerical results can predict it accurately. A discussion of two different methods to compute the pressure drop is given, showing the differences in relation to the airflow characteristics near the outlet of the diffuser.

1. Introduction

Computational Fluid Dynamics (CFD) is an useful tool for designing and testing industrial devices such as wings and planes, heat exchangers for electronic devices or Heating, Ventilation and Air Conditioning (HVAC) diffusers among others. Although CFD allows engineers a proper design of terminal devices, real testing is required through experiments because it uses turbulence modeling for applied problems. In fact, the parameters of the turbulent models must be tuned by comparing numerics with a given experiment even though their final values are often used for other cases or geometries.

Researchers have been mostly interested in predicting airflow patterns in rooms, which reveals the optimal position of diffusers and return grilles for HVAC applications [1]. Regarding the evaluation of ventilation performance in buildings, we identify seven types of models: analytical, empirical, small-scale experimental, full-scale experimental, multizone network, zonal and CFD [see [2,3], for a review on the subject]. In the last years, CFD has become increasingly popular due to the increase in computational power of personal computers, allowing the simulation of problems that were impossible to solve a few years ago. Now simulations of the flow inside an office [4], an entire building such as a train-station [5] or even the contaminant transport inside an aircraft cabin can be performed [6]. To achieve accurate numerical results which are a quite time consuming task, different scales must be taking into account resulting in complicated meshes. A desirable and useful computational tool for HVAC designing should solve a simple case on a personal computer in a reasonable time. The accuracy and the speed of the simulations are controlled by the size of the mesh, the turbulent model used and the numerical technique employed to solve the equations. In the last two aspects, less progress can be made. As for the turbulence modeling, the $k-\varepsilon$ algorithm, which has been widely used for HVAC applications [7–10], has been tested against experiments. Other procedures such as one equation models [11], or $k-\varepsilon$ Re-Normalisation Group (RNG) methods yield better results in some specific cases [9,12,6]. In addition, solvers are usually based on the SIMPLE algorithm (Semi-Implicit Method for Pressure Linked Equations) [13], which is a steady-state solver for turbulent Navier–Stokes (N–S) equations. New solvers compute linear systems that arise when discretizing N–S equations using the Algebraic MultiGrid (AMG) procedure, which proves to be one of the quickest methods to solve a linear system of equations iteratively. New methods that are less accurate than the present one have appeared in recent years such as the Fast Fluid Dynamics (FFD) model [14] that provide a speedup of 50 over standard solvers. It can be used on GPUs (Graphic Cards) to speed up the simulations

* Corresponding author. Universidad de Málaga, E.T.S., Ingenieros Industriales, 29071 Málaga, Spain. Tel.: +34 951 952 383.
E-mail address: lparras@uma.es (L. Parras).

http://dx.doi.org/10.1016/j.buildenv.2014.05.001
0360-1323/

Nomenclature

β	thermal expansion coefficient (1/K)
ε	turbulent dissipation (m^2/s^3)
κ	turbulent kinetic energy (m^2/s^2)
A_0	total opening area (m^2)
A_{eff}	effective area (m^2)
A_{free}	free area (m^2)
Ar	Archimedes number (−)
P	absolute pressure (Pa)
p	thermodynamic pressure (Pa)
Q	flow rate (m^3/h)
T_0	ambient temperature (K)
K_a	constant for the specific inlet device (−)
T_i	supply air temperature (K)
U	supply air velocity (m/s)

ten times more as it has been shown recently by [15]. To sum up, the solution to reduce the time to obtain a good estimation of the flow inside the inhabited region using CFD methods is to avoid modeling the small details of the real problem, e.g. the interior of the diffusers or the exact shape of the objects inside a room.

Consequently, in this work we present a way of reducing the size of the problem using a modeled boundary condition for diffusers. In other words, a difficult problem is split into two different simulations, the outflow of the terminal device being the input condition of the room.

A first approximation to model a diffuser is to replace it with a rectangular slot of area A_0, this surface being the total opening area of the diffuser where we impose all the values required for numerical simulations: velocity and temperature fields, together with turbulent airflow characteristics. This approximation works for a very simple diffuser without perforated faces or vanes. Otherwise, the airflow goes through a free area A_{free} that is smaller than the total area A_0. For this reason, A_{free} is defined as "the sum of the smallest areas of the cross section of all openings of the air terminal devices" [16]. Thus, the area defining the flow rate is called the effective area, A_{eff}, or "the smallest net area of an air terminal device utilized by the air-stream in passing through the air terminal device" [16]. However, there are some uncertainties in defining the exact value of the uniform velocity at the inlet diffuser when flow rate Q is imposed. So the real problem is to determine A_{eff}, which is from 10 to 40% smaller than A_{free}. The simple method described above is known as the *basic model* [17], which has proved to be not good enough to estimate properly the throw and drop for non-isothermal applications [18].

An improvement to this *basic model* is the momentum method [18], which de-couples the momentum and mass boundary conditions for the diffuser in a CFD simulation. Flow velocity U_0 (modulus and direction), A_{eff} and the flow rate must be measured, the recommendation being to measure the flow velocity in nine points near the diffuser so as to obtain the direction of the flow from smoke visualizations [19]. Another method [11] is an N-point air-supply opening model that reduces the number of points in the simulation and gives accurate results. This method has proved accurate for displacement ventilation diffusers, square ceiling, round ceiling, vortex ceiling and grille [20].

The box method [1], which represents the boundary conditions in an imaginary box around the diffuser, was developed by Nielsen. All the variables must be imposed (measured) on the plane parallel to the plane of the diffuser slot and the normal derivative of the variables should be nil on the other surfaces [1]. Besides, boundary values of the variables must be obtained by mass and energy conservation equations applied to the box [19]. This powerful method can use three types of data: experimental measurements to impose the velocity field [19,20], analytical correlations [1,8] or simulated parameters, as has been done recently [21]. One drawback of this method, however, is to determine the size of the box, and another is that it is not suitable for low Reynolds numbers. This method has proved accurate for all kind of diffusers except for displacement ventilation [20] because in these low velocity diffusers the buoyancy effects are quite important near the outflow.

Another improvement to the basic model is the *Prescribed Velocity Method* (PV-method) [1,22] which was also developed by Nielsen by defining additional velocity values near the diffuser. Its drawbacks are that a set of experiments have to be carried out for the test of any diffuser with respect to the box Method and that these measurements cannot be extrapolated to different diffusers. The PV-method has the advantage of reducing the number of measurements to parametrize an analytical near-wall jet flow that can be prescribed directly with very accurate results [22,23].

More recently Zhang et al. [24] proposed a new method for displacement diffusers where flow conditions are specified on cells over the simplified diffuser geometry. The flow values are imposed on several cells randomly distributed on the diffuser surface whereas the rest remain closed. The ratio of opened cells must be equal to the effective area. It has the advantage that it can easily be implemented in commercial CFD software but on the other side, the effective area as other inlet parameters as turbulent properties or flow direction, have to be obtained experimentally.

Finally, the improvement on the computer capacity allows full simulations of diffusers, which were first pointed out as a possible solution [1] and have been already performed in recent years [25,21]. Numerical simulations using Micro/Macro Level Approach (MMLA) [21] present some discrepancies due to the unstable behavior of the airflow whilst velocity profiles behave similarly to the experimental ones.

In this paper we propose the opensource code *OpenFOAM* [26] to solve the flow inside the diffuser, and then use this result as the inlet of the numerical test room. With this MMLA-like approach [21] we compare global experimental data such as the shape of the visible cold plume. We also map turbulence properties as κ and ε. Furthermore, we use flow visualizations which are quicker and easier to set up than hot-wire anemometry or particle image velocimetry (PIV). Experimental data confirm that our numerical results are reliable. Finally, we add the analysis of the values for pressure drop in the air terminal device, which is important in designing the air-duct system.

The paper structure is as follows. In Section Section 2 the diffuser is presented together with the experimental setup and instrumentation. In Section Section 3 we first compare numerical and experimental results. Once validated, we obtain from numerical simulations the pressure drop and the throw and drop of the plume. Finally, we draw some conclusions in Section Section 4.

2. Formulation of the problem

This study corresponds to the diffuser named RDHV 500 × 150 and manufactured by ALTRA S.L. in Málaga (Spain). The 3D CAD picture of the diffuser is shown in Fig. 1(a). It consists of a rectangular grille inserted in a square-section duct of 500 mm and 150 mm in the horizontal and vertical directions, respectively. The grille has 6 vanes in the horizontal direction and 19 in the vertical [see Fig. 1(b)], all of them always aligned with the flow direction, so that the treated cool airflow is parallel to them. The gap surface between vanes was small (near 20 × 20 mm^2), so the mesh must be extremely fine in this part of the diffuser. The measured A_0 was

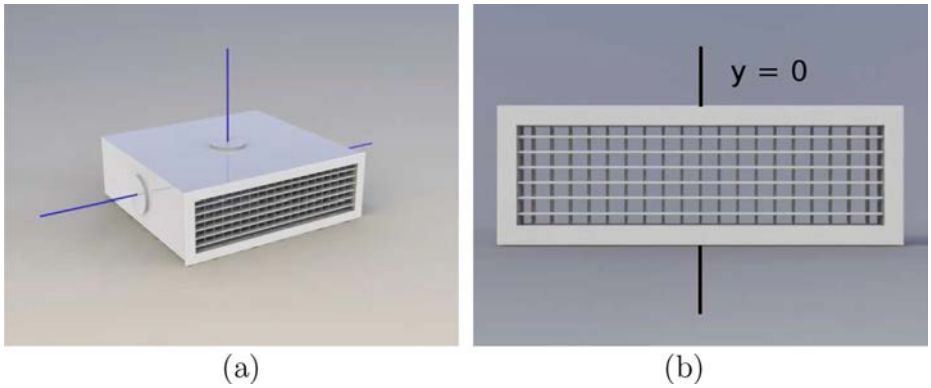

Fig. 1. (a) Computer model of the air terminal device (diffuser) RDHV 500 × 150 with the position of the measurements points for the pressure and (b) a frontal image of it.

approximately 0.0624 m^2 and the free area, $A_{free} \approx 0.0441$ m^2. As has been stated in the previous section, two studies are reported in this paper: the throw and drop of the airflow and the pressure drop produced by this diffuser, experimentally and numerically. Both studies are complementary, and they will help us study and design future air terminal devices.

2.1. Experimental setup

The experimental setup is shown in Fig. 2. The treated air was moved by a fan and its rotation speed was controlled by a frequency converter. The air was led to a square-section insulated duct (500 × 150 mm) of 5 m long through a flexible circular duct of 150 mm diameter. The purpose of the 5 m-long square duct was to stabilize the flow and to reach a constant velocity profile near the diffuser. To measure the velocity/flow rate inside the duct a hot-wire anemometer was inserted 1 m before the diffuser, at the middle section of the duct. This position was selected following two criteria: firstly, far enough from the connection of the circular duct to the square-section duct so the airflow was uniform without perturbations, and, secondly, far enough away from the diffuser to avoid any influence in the measurements. The velocity was measured for different heights inside the duct showing a nearly constant velocity profile. The inflow air temperature (T_i) right at the beginning of the duct and room temperature (T_o), far away from the diffuser, were measured with a PPT-100 temperature sensor. The room in which the experiments were carried out in ALTRA labs was 25 m long, 5 m wide and 3 m high. The diffuser and the duct were located to set the lower part of the diffuser at a height of 2.25 m from the floor.

A differential pressure transducer Dwyer DH3-004 has been used to measure the pressure drop. The low pressure tube measures the average pressure of three points fixed to the surface of the diffuser duct: on the upper surface and on both sides, left and right [see the tubes and an example of the connection in Fig. 1(a)]. These three points were located 10 cm before the vanes. Several configurations have been tested for the measurement of the low pressure while the high pressure was connected to the ambient. If the flow is uniform and steady at the diffuser inlet (with no recirculation regions), all the configurations provide the same results. Previous tests with shorter duct lengths have given less accurate results.

To make the flow visible, a smoke generator has been designed and built [27]. A compressor was used to introduce high pressure air through an end blocked tube with two small holes on the side immersed in olive oil. This is a non-intrusive experimental technique that produces small drops of oil (1 μm average diameter) and is used for flow visualization [28] or to seed the air to use PIV or LDA (Laser Doppler Anemometry). The quantity of olive oil drops can be controlled by using a bypass air on the device and due to their small size they follow the flow accurately. The sedimentation velocity was calculated to be less than 1 mm/s, and we have also checked that for isothermal jets the plume was horizontal. To obtain instant

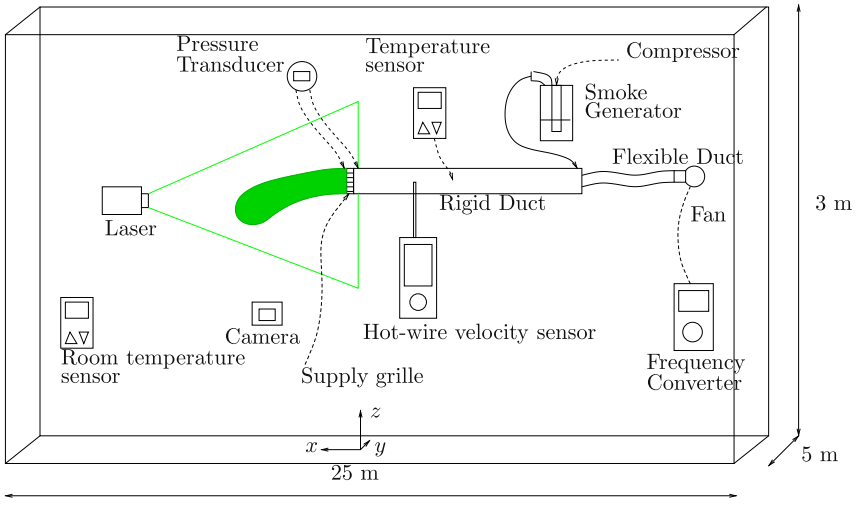

Fig. 2. Sketch of the experimental setup.

pictures, the flow was illuminated by a 2 W solid state laser. To generate the laser sheet cylindrical lens were used and they were later aligned to obtain the flow visualization in the (x, z)-plane (see Fig. 2). Two mirrors aligned to the main laser sheet have been used to increase the field of view. It has been checked that the air introduced by the smoke generator was lower than 0.3% of the total flow rate, Q. A digital HD camera at 25 frames per second with a resolution of 1080 $\times$ 1920 pixels was used to record the videos.

2.2. Numerical setup

One of the main advantages of the numerical simulations for HVAC applications is the possibility of designing and testing a device without manufacturing it. Although better and complex CFD codes have been developed in the last decade, one can not ensure accurate results until they are compared with experimental data. Two different problems were studied: the pressure drop and the airflow generated by the diffuser. For the first problem, the diffuser is set in the middle of a square duct 40 cm in length. The domain was divided in three parts: the inflow region, the vanes of the diffuser and the outflow section (see Fig. 3). The inflow and outflow sections were meshed with hexahedrons, decreasing the size of the mesh in the x direction when they approach the diffuser section. This section was divided into two regions, one for the horizontal vanes and other for the vertical vanes. Both regions were meshed with prisms and tetrahedrons with typically edge size of 0.5 mm. Only half of the domain was meshed due to the symmetry with respect to $y = 0$ as shown in Fig. 1(b).

For the second problem, instead of solving the diffuser and the room at the same time, we split the numerical domain into two parts in order to reduce the cost of the numerical simulation. This has been done recently by Cehlin and Moshfegh [21] for displacement diffusers. The idea is to generate two meshes, one for the diffuser and the other for the room, and set the inlet boundary conditions for the room as the outlet boundary conditions for the diffuser. The first mesh is the one used to analyze the diffuser. The meshing method is similar to the one presented above for the pressure drop. The inlet region has an hexahedral mesh and the region of the vanes has been meshed by prisms and tetrahedrons [see Fig. 4(a) and (b)]. The outlet boundary conditions are set at 1 mm from the vanes of the diffuser as shown in Fig. 4(a). The velocity field presents a checkerboard shape due to the wake generated by the horizontal and vertical vanes as can be observed in Fig. 4 (b). In addition, a room of 4 m long, 2.5 m wide and 3 m high was created and meshed with a coarser hexahedral grid (see Fig. 5). The inlet velocity field and other variables such as the temperature or turbulence properties were mapped from the results at the outflow of the diffuser mesh. We supposed symmetry with respect to $y = 0$ in the problem to solve only half of the domain. Typical mesh sizes are about 1.3 million grid points for the diffuser [Fig. 4(b)] and 1 million grid points for the room (Fig. 5). The number of points in the diffuser outflow boundary condition is 6370 and in the room inflow boundary condition 312 so there is a reduction of 95% in the number of points. This value is high enough to describe all the characteristics of the airflow. As it will be shown later, this method is quite useful for designing new diffusers because it provides reliable results in a reasonable short period of time (several minutes for the diffuser mesh and several hours for the room mesh, run on 8 processors on a workstation). Besides, a grid convergence study was carried out. To this end, we decreased the characteristic length of the mesh while keeping the same meshing method to reach a final mesh with an increase of 20% in the number of points. Results between the fine and coarse meshes

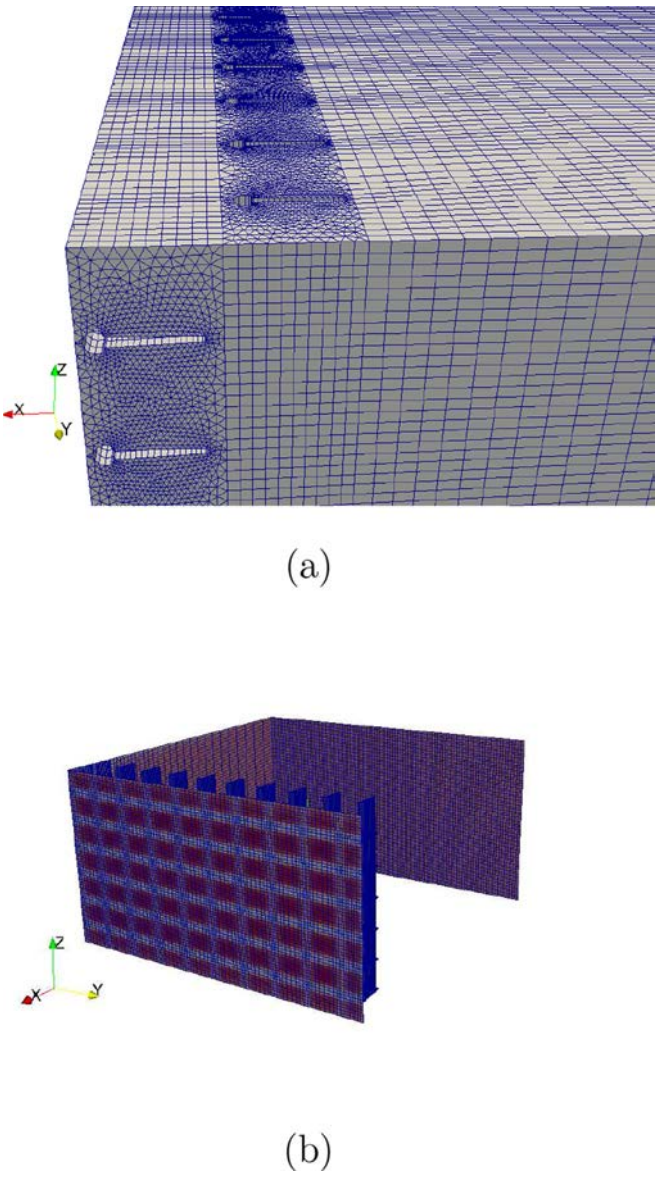

Fig. 4. (a) Mesh detail of the diffuser and (b) velocity magnitude at the outflow of the diffuser.

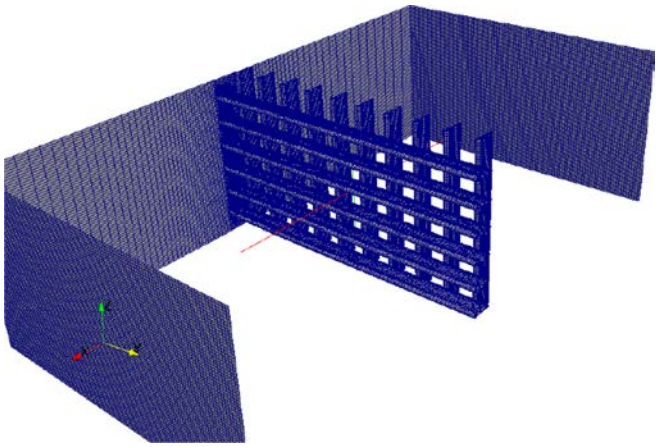

Fig. 3. Mesh detail of the diffuser for the analysis of the pressure drop.

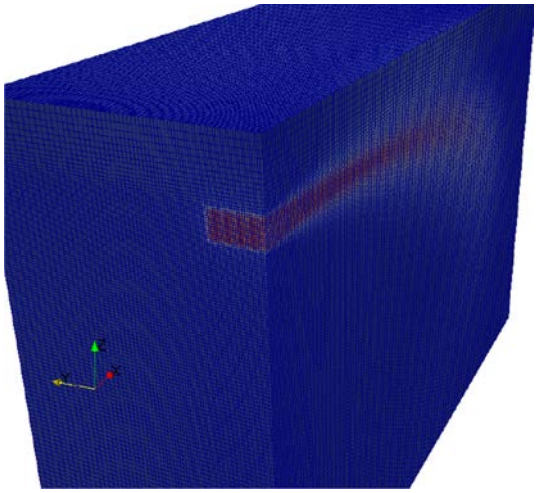

Fig. 5. Mesh of the room with the velocity magnitude taking into account the inflow of the diffuser.

vary less than 1% in terms of the velocity field. All the meshes have been generated by GAMBIT®.

As for the boundary conditions in the meshes of the diffuser (one generated for the pressure drop and the other generated for the airflow distribution) we imposed a uniform velocity field at the inflow, together with non-slip velocity conditions in all the walls and the vanes, symmetry boundary conditions in the symmetry plane ($y = 0$) and zero gradient of the velocity field at the outflow. The temperature in the whole spatial domain was constant and equal to T_i. In the room mesh, slip-velocity conditions on the ceiling and lateral walls to avoid the Coanda effect were imposed, with a constant temperature value of T_0. In addition, the boundary conditions were non-slip and constant temperature T_0 on the floor and the wall in which the diffuser was placed except the region of the outflow of the terminal device (see Fig. 5). Finally, zero gradient for the velocity field at the outflow of the room was set.

The problem was solved with *OpenFOAM* [26] using a turbulent steady-state solver for the diffuser (*simpleFoam*) and a Boussinesq turbulent, long-time step unsteady solver for the room (*buoyantBoussinesqPimpleFoam*). The turbulent model used in this study is $\kappa-\varepsilon$ model, which is a two equation turbulence model, in which the turbulent viscosity depends on the turbulent kinetic energy κ and on the turbulent dissipation ε. The implementation of this method is detailed in [26]. The exact model that OpenFOAM uses was initially developed by Launder and Sharma for turbulent heat transfer in a spinning disk [29]. We show below that for numerical non-isothermal cases, there is a good agreement with the experimental data.

3. Results

The throw and drop as well as the pressure drop of the air terminal diffuser are the main results discussed in this section.

3.1. Comparison between numerics and experimental data

To ensure reliable numerical data, used the shape of the flow plume for different flow rates $Q = 90, 170, 260$ and $350\ \mathrm{m^3/h}$ and a constant value of temperature difference $\Delta T = T_o - T_i = 6$ K. To this end we recorded the flow in the streamwise direction, (x,z)-plane for 1 min at 25 fps (frames per second) for a given experiment. Instantaneous pictures were later obtained such as the one shown in Fig. 6(a). It can be observed how the cold air flows out of the diffuser with oscillations due to turbulence patterns and how the plume drops to the floor due to buoyancy. Only the region near the terminal device could be observed as a consequence of the limitations in the field of view. In addition, when the concentration of oil droplets diminish, the scattering of the laser beam is reduced and the images have less light intensity and contrast. In this work, a

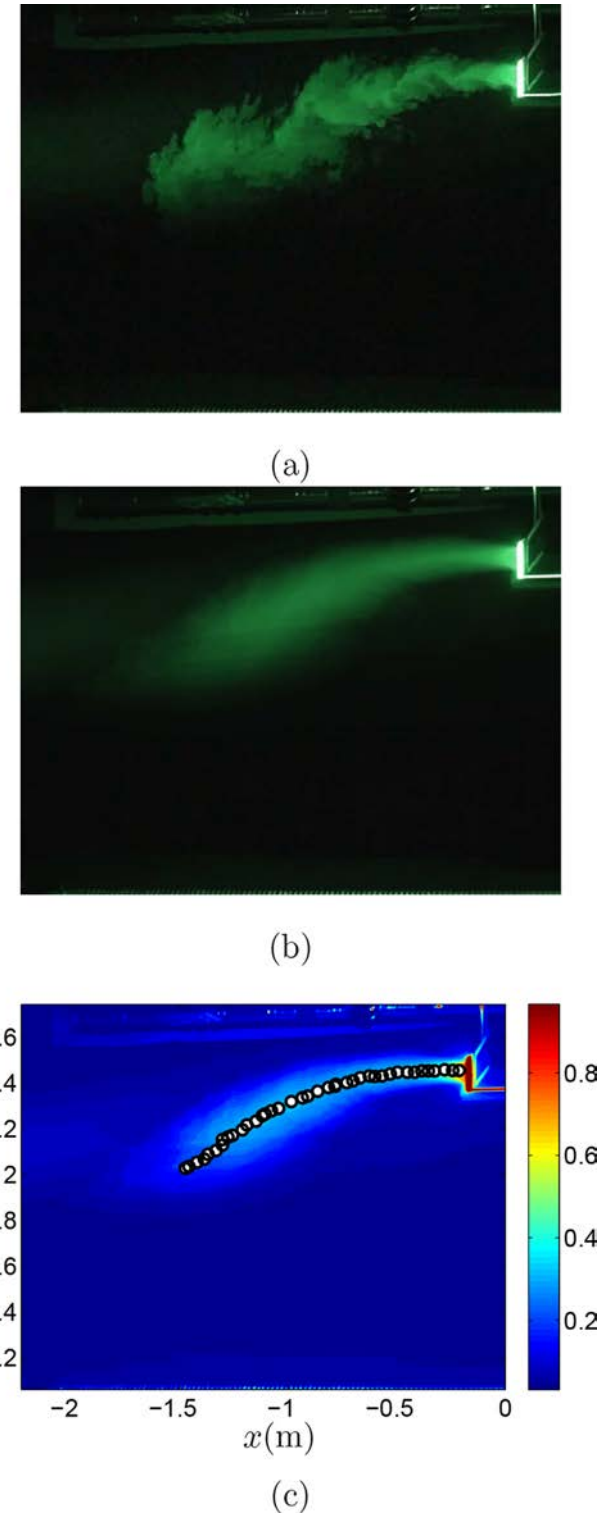

Fig. 6. (a) Instantaneous image of the flow produced by the diffuser, (b) mean image of the flow and (c) intensity of light of the mean image. All the images are taken from the case $Q = 260\ \mathrm{m^3/h}$.

compromise between the field of view and the light intensity was adopted. We later computed the average image using Matlab for all the pictures of each experiment [see Fig. 6(b)] and so were able to estimate the mean airflow pattern of the oil drops inside the room. Previous works on the same subject have performed flow visualizations inside a test room to see qualitatively only the characteristics of the jet [30] and to obtain images as the one presented in Fig. 6(a). Hence, we show how simple visualizations can be used to characterize the jet emerging from the diffuser quantitatively.

To obtain quantitative data for each experiment, the flow has been calibrated with an object of 2 m size giving errors between 2 and 5 mm/px. The mean image has 1080 × 1920 pixels, with a color depth of 8 bits [see Fig. 6(b)], so we are able to represent the light intensity of the image as it is depicted in Fig. 6(c). This procedure allows us to determine the maximum light intensity through the image, following the line of the center of the flow (x_c, z_c). These points are also shown with circles in Fig. 6(c). If the same process is repeated for all the cases studied the results shown in Fig. 7 are obtained. Numerical results of the temperature isocontours for different flow rates are plotted in (a), (c) and (e), together with the experimental centerline. Figures (b), (d) and (f) represent the experimental isocontours of light intensity with the centerline path. A reasonable good agreement is observed between the numerical and the experimental data. To compare CFD and flow visualizations we assumed that the oil concentration is maximum at the inflow of the diffuser (as happens for the numerical temperature field). Both the numerical temperature and the oil concentration fields must behave in the same way due to the fact that in this problem diffusion is dominated by turbulence. It is worth mentioning that this assumption is not entirely justified if the experimental and numerical isocontours are observed in detail. The light intensity of the droplets seems to have a steeper slope than the temperature field as one moves away from the centerline path. This means that the turbulent thermal diffusivity in the numerical code is greater than the mass turbulent diffusivity of the oil droplets. In this case, the inertial terms become the leading ones here, thus making the comparison reliable.

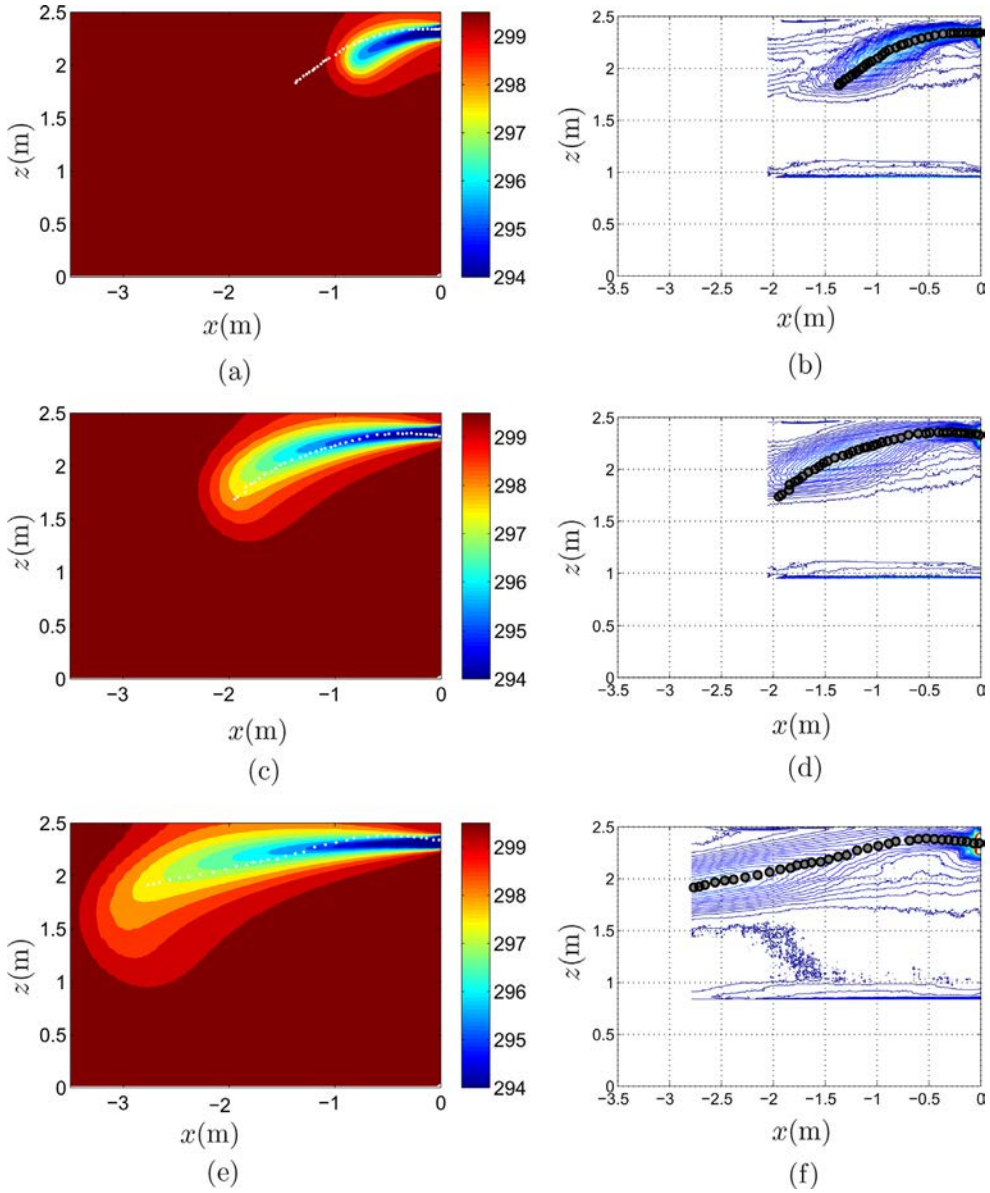

Fig. 7. Mean images of the smoke visualization, together with the numerical contours of the temperature field and its comparison with the position of maximum concentration of oil drops for $Q = 170$ (a)–(b), 260 (c)–(d) and 350 m^3/h (e)–(f), respectively.

To double-check our experimental results we present in the same figure all the centerline results, compared with previous results in the bibliography. Nielsen in [22] confirmed that the coordinates of the center of the plume (x_c, z_c) [see Fig. 6(c)] must follow the following expression (taken from [31])

$$\frac{z_c}{\sqrt{A_0}} = 0.6\frac{Ar}{K_a}\left(\frac{x_c}{\sqrt{A_0}}\right)^3, \tag{1}$$

where K_a is a constant depending on the diffusers and Ar the Archimedes number, defined as

$$Ar = \frac{\beta g\sqrt{A_0}\Delta T}{U_0^2}, \tag{2}$$

where β is the coefficient of thermal expansion in air and g the gravity acceleration. In this research, x is the axial distance from the center of the diffuser and y is the vertical distance to the center of the diffuser (see Fig. 2).

The experimental and numerical results collapse following the expression:

$$\frac{z_c}{\sqrt{A_0}} = 0.6\frac{Ar^n}{K_a}\left(\frac{x_c}{\sqrt{A_0}}\right)^2, \tag{3}$$

Fig. 8 represents by a dashed line the nondimensional absolute value of the vertical coordinate z_c with the estimation of equation (3) together with the numerical and experimental results, fitted with the same expression for $x_c/\sqrt{A_0} \geq 2$ being $n = 0.8765$ and $K_a = 1.366$ for the experimental measurements and $n = 1.3246$ and $K_a = 0.2741$ for the numerical data. It can be observed how experimental centerlines obtained by the image processing and numerical results collapse in the nondimensional variables over the theoretical prediction. However, experimental results present great dispersion at high nondimensional distances from the diffuser. This fact can be explained because the x-velocity of the flow attains the same order of the z velocity, so the airflow is no longer dominated by inertia and drops vertically. Nevertheless, two small discrepancies arise here in comparison to Koestel's prediction, equation (1), n is not equal to 1 and the exponent for $x/\sqrt{A_0}$ is 2 not 3. Regarding the coefficient n, the results from CFD and experiments gave us an estimation around $n = 1$ so there is a reasonable good agreement. The exponent of $x/\sqrt{A_0}$ has a quadratic dependence that appears both in experiments and simulations. Koestel [31] obtained analytically his expression for jets, which has $dz_c/dx_c \ll 1$, which is not the case for the diffuser jets studied here. Other references provide different laws of decay with the distance [32] and, particularly [33] and [34] confirm a quadratic decay. Once we have tested the numerical simulations, we will introduce the results for the pressure drop in the terminal device and the throw and drop of the diffuser airflow.

3.2. Pressure drop

As stated above, the pressure drop on this device has also been measured experimentally. We have been measuring the static pressure at point p_i, due to the fact that the pressure tube was inserted at the surface. The second pressure tube was left open to the atmosphere and at the same height as the center of the diffuser, obtaining the static pressure outside p_o. In this case, we measured the static pressure drop in the diffuser instead of the head loss

$$\Delta P = p_i + \frac{1}{2}\rho U_i^2 - p_o - \frac{1}{2}\rho U_o^2, \tag{4}$$

where subscripts i, o refer to inlet and outlet respectively and ρ being the density. We suppose that $U_o \approx 0$ in the last equation for the experimental calculation and uniform variables in each section, so U_i is known with the relation between the flow rate Q and the total area A_0. We performed the same study numerically following two different methods. The first consists in sampling the variables p and U on a line that belongs to the symmetry plane of the diffuser, located in the middle of its height. In Fig. 9 the pressure and the velocity fields are shown on this line for $Q = 170$ m^3/s. The position of the diffuser corresponds to $x = 0$. It can be observed how the pressure was reduced at that position, and an increase in the velocity is also noticed due to the reduction of section for the presence of the vanes. The pressure drop can be calculated from these numerical data by applying its definition, and taking the value between the inlet and the outlet section, so it reads as

$$\Delta P = p(x=-0.2) + \frac{1}{2}\rho_i U(x=-0.2)^2 - p(x=0.2) - \frac{1}{2}\rho U(x=0.2)^2. \tag{5}$$

However, the method described above has a drawback: the selection of the line where the pressure is measured. Different lines will probably produce slightly different results. If one only takes into account the pressure and velocity at the inflow and

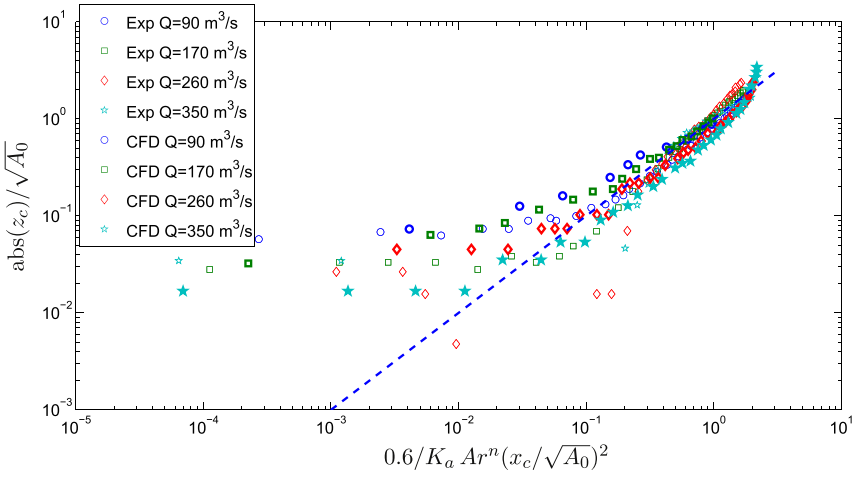

Fig. 8. Experimental plot of the centerline of the plume for different flow rates. CFD results are in thick line symbols.

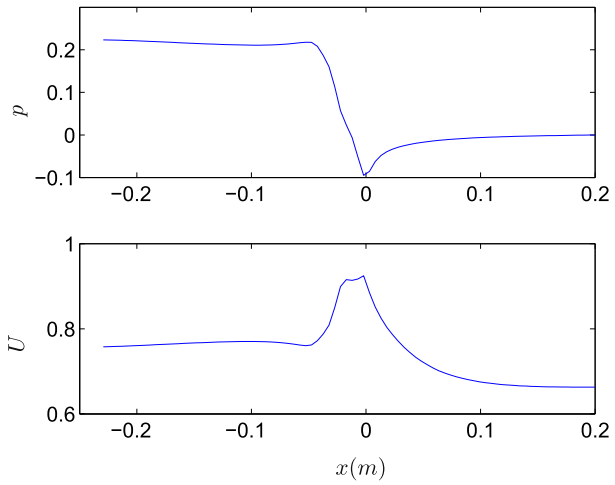

Fig. 9. Pressure and velocity field trough the line perpendicular to the plane defined the two symmetry planes of the diffuser.

outflow sections of the computational domain (shown in Fig. 10), the mean value can be defined by the integration of the following equation,

$$\Delta P = \frac{1}{A}\int_{yz}\left(p_i + \frac{1}{2}\rho U_i^2 - p_o - \frac{1}{2}\rho U_o^2\right)dydz, \tag{6}$$

A being the area where we compute the integral. In Fig. 10 it can be observed how the flow has an almost constant axial velocity at the inflow (except for the boundary layers) and once it has passed trough the vanes, the flow accelerates in the new free area whereas it just decelerates down the vanes, giving the characteristic checkerboard velocity profile.

The results given by (5) and (6) are plotted in Fig. 11. Experimental data, the computation of the line method and the calculation with the integral method are depicted in circles, dash and solid lines, respectively. One observes reasonable good agreement in comparison with the numerical results. This small difference can be explained by the experimental errors. The pressure transducer is a 0–100 Pa measurement device, with an accuracy of 0.1 Pa, that is of the order of magnitude of what we are measuring at low flow rates. We see how the integral results are quite accurate for high flow rates, in which the values of the pressure drop are at least ten times the resolution of the transducer. It is also worth mentioning that in this pressure drop study we selected new flow rates to compare the experimental results beyond the results given for the plume ($Q = 440$ and 530 m^3/h).

3.3. Throw and drop of the airflow

ASHRAE [35] defines throw T and drop D as the maximum longitudinal and minimum vertical distances where the airflow has constant values of the velocity magnitude. We have adopted the same definition in this work. Fig. 12 shows the isocontours of the velocity magnitude in the symmetry plane, which corresponds to a given velocity magnitude. The points defining the throw and drop for each flow rate are marked in circles and squares for velocity magnitudes of 0.1 m/s and 0.25 m/s respectively.

Once the results were obtained, the values of the throw and the drop are presented in Fig. 13. $T0.25$ and $D0.25$ represent the throw and drop of the diffuser for a magnitude of the velocity field of $|u| =$ 0.25 m/s and $T0.1$ and $D0.1$ represent the throw and drop of the diffuser for a magnitude of the velocity field of $|u| = 0.1$ m/s. It can be observed how the throw is almost linear with the flow rate. It

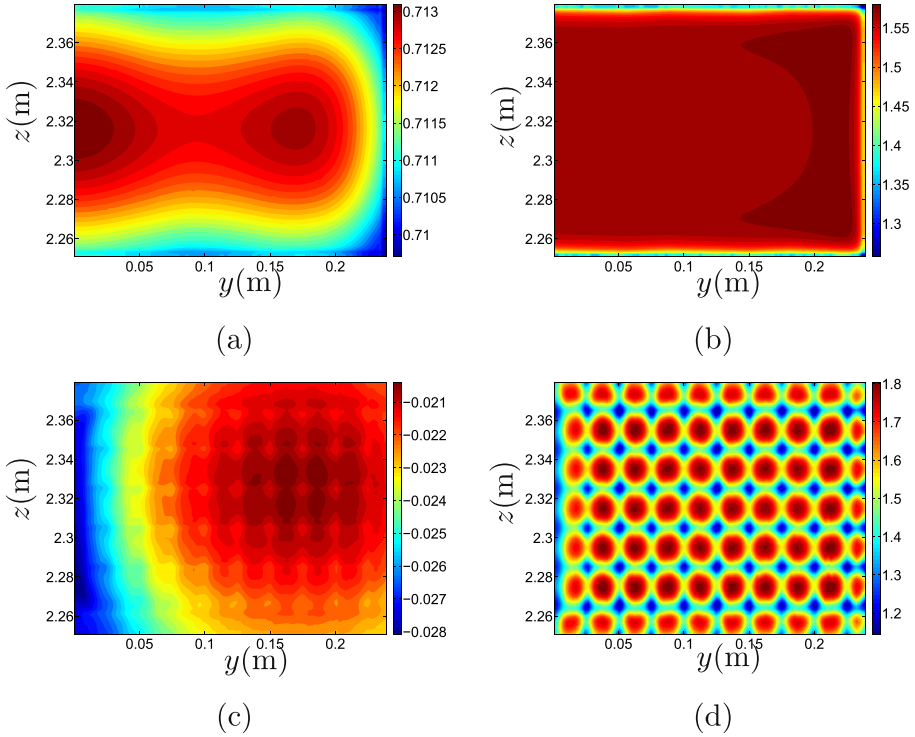

Fig. 10. (a) Pressure and (b) velocity fields at the inlet of the domain and (c) and (d) the same fields at the outlet of the domain for $x = -20$ cm in (a)–(b) and $x = +20$ cm in (c)–(d). $Q = 350$ m^3/h, pressure and velocity, given in Pa and m/s respectively.

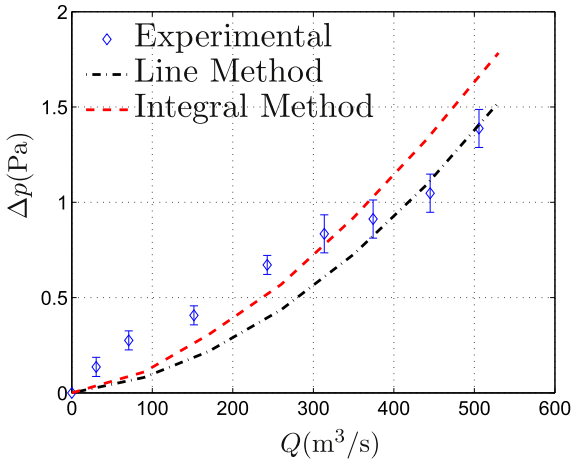

Fig. 11. Pressure drop on the diffuser. On circles the experimental results, on dashed line the line method and on dash-dot line the integral method.

would be expected that the greater the flow rate is, the larger the effect of the spread on the *y* direction which would help to reduce the throw, reaching a saturated state. Nevertheless, this was not checked in this study due to limitations in the size of the room meshes. On the other hand, the drop reaches a saturation value before the throw and it can be also observed how the airflow spreads in the *y* direction, so it reduces the maximum vertical distance that the plume can reach.

4. Conclusions

In this paper we have developed a method of studying the characteristics of an HVAC diffuser with CFD and experiments. We have used experiments to visualize the fluid flow by introducing oil droplets, which allows us to check the accuracy of the numerical simulations. This method is less precise than measuring the real flow using PIV or hot-wire anemometry, but easier to setup and analyze since the only experimental devices required are a laser and a digital camera. It has been stated that only one measurement of the velocity field inside the duct is required to obtain the airflow rate and some image processing. Reasonable good agreement was found between the temperature field obtained by numerical simulations and the experimental data of the plume shape.

A method of numerically solving the fluid flow was developed. This procedure separates the fluid flow into two linked problems. Firstly, the numerical problem inside the diffuser was solved with a very fine mesh due to the presence of boundary layers near the vanes, and secondly the airflow was determined on a coarser mesh in the room. The connection between the two problems lies in the fact that all the variables at the outflow of the diffuser are set as the inlet variables of the room problem. This speeds up the calculations and good agreement can be found between experimental results and numerical data, the source of small errors being the limitations of the experimental technique and the number of pixels of the camera. Besides, this method allows us to map turbulence properties that are usually estimated on the box method or the PV-method. It has been shown that the equation that governs the shape of the plume is different from those presented in literature [31]. We have shown that other authors predicted a quadratic flow with other conditions, as the results presented in the paper. In addition, from the numerical results we computed the throw and drop of the diffuser, which are significant parameters for designing. The drop shows a saturation in its maximum value, the explanation of which is the movement of the airflow in the transverse direction.

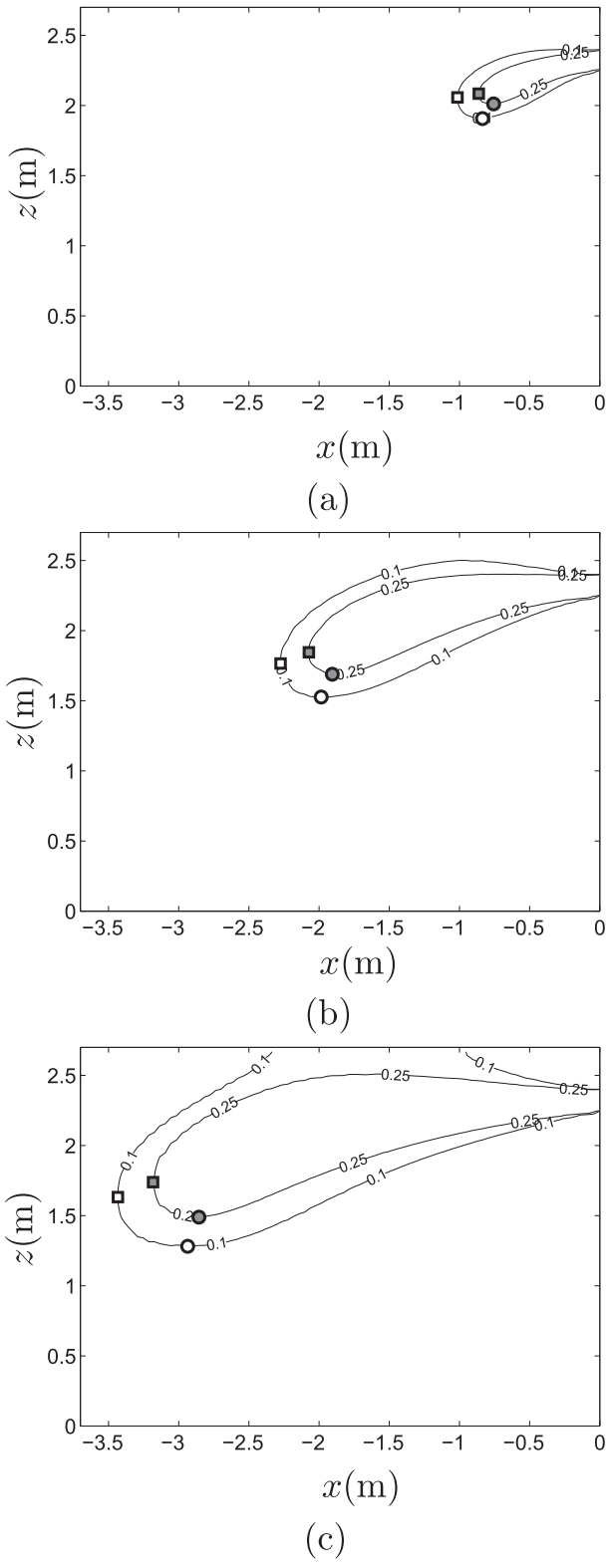

Fig. 12. Numerical contour of velocity magnitude in the mid plane. In squares are marked the points that fixed the throw and in circles the drop. White markers are for $|u| = 0.25$ m/s and gray markers for $|u| = 0.1$ m/s, (a), (b) and (c) for $Q = 170{,}260{,}350$ m^3/h respectively.

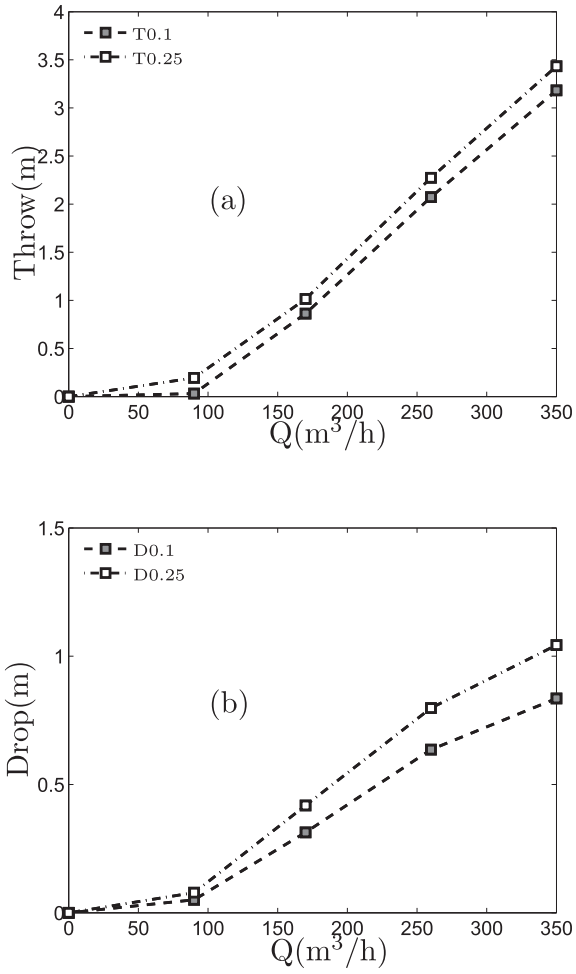

Fig. 13. (a) Throw and (b) drop versus the flow rate for different magnitudes of the velocity field.

Finally, we have also shown that we can reproduce the results for the pressure drop in the diffuser, another important parameter for designing airflow distribution systems. We have distinguished the effect of the air loss of kinetic energy discharging in a room with the effect of the vanes in the diffuser, comparing numerical results and experimental data. The integral method allows us to obtain a mean pressure drop in the air terminal device by taking into account the vane geometry which gives a better estimation than the line method for higher flow rates.

Acknowledgment

The authors are thankful for the financial support from ALTRA through the project ENERFACE 13/641. The authors thankfully acknowledge the computer resources, technical expertise and assistance provided by the SCBI (Supercomputing and Bioinformatics) center of the University of Malaga. We also thank Miguel García Arreza his useful comments.

References

[1] Nielsen P. Representation of boundary conditions at supply openings; 1989. Technical report, IEA, Annex 20, Research item 1.11.
[2] Chen Q, Lee S, Mazumdar K, Poussou S, Wang L, Wang M, et al. Ventilation performance predictions for buildings: model assessment. Build Environ 2010;45:295–303.
[3] Chen Q. Ventilation performance predictions for buildings: a method overview and recent applications. Build Environ 2009;44:848–58.
[4] Corgnati S, Perino M, Fracastoro G, Nielsen P. Experimental and numerical analysis of air and radiant cooling system in offices. Build Environ 2009;44:801–6.
[5] Li Q, Yoshino H, Mochida A, Lei B, Meng Q, Zhao L, et al. CFD study of the thermal environment in an air-conditioned train station building. Build Environ 2008;65:118–31.
[6] Liu W, Wen J, Lin C, Liu J, Long Z, Chen Q. Evaluation of various categories of turbulence models for predicting air distribution in an airliner cabin. Build Environ 2013;65:118–31.
[7] Gan G. Evaluation of room air distribution systems using computational fluid dynamics. Energy Build 1995;23:83–93.
[8] Hue Y, Haghighat, Zhang JF, Shaw C. A systematic approach to describe the air terminal device in CFD simulation for room air distribution analysis. Build Environ 2000;35:563–76.
[9] Djunaedy E, Cheong K. Development of a simplified technique of modeling four-way ceiling air supply diffuser. Build Environ 2002;37:393–403.
[10] Luo S, Heikkinen J, Rouxa B. Simulation of air ow in the IEA Annex 20 test roomvalidation of a simplified model for the nozzle diffuser in isothermal test cases. Build Environ 2004;39:1403–15.
[11] Zhao B, Li X, Yan Q. A simplified system for indoor airflow simulation. Build Environ 2003;38:543–52.
[12] Posner J, Buchanan C, Dunn-Rankin D. Measurement and prediction of indoor airflow in a model room. Energy Build 2003;35:515–26.
[13] Patankar SV, Spalding D. A calculation procedure for heat, mass and momentum transfer in three-dimensional parabolic flows. Int J Heat Mass Transf 1972;15:1787–806.
[14] Liu W, Long Z, Chen Q. A procedure for predicting pressure loss coefficients of duct fittings using CFD (rp-1493). HVAC&R Res 2012;18:1168–81.
[15] Zuo W, Chen Q. Fast and informative flow simulations in a building by using fast fluid dynamics model on graphics processing units. Build Environ 2010;45:747–57.
[16] ISO 5219 Nielsen P. Air distribution and air diffusion-laboratory aerodynamic testing and rating of air terminal devices. Technical report. International Organization for Standardization; 1984.
[17] Modeling of a supply air terminal for room air simulation. In: Proceedings of the 12th AIVC conference; 1991.
[18] Simulation of a multiple-nozzle diffuser. IEA Annex 20 Subtask 1 Research Item 1.20. In: Proceedings of the 12th AIVC conference; 1991.
[19] Xrebric J, Chen Q. A method of test to obtain diffuser data for CFD modeling of room airflow. ASHRAE Trans 2001;107:108–16.
[20] Xrebric J, Chen Q. Simplified numerical models for complex air supply diffuser. ASHRAE Trans 2002;8:277–94.
[21] Cehlin M, Moshfegh B. Numerical modeling of a complex diffuser in a room with displacement ventilation. Build Environ 2010;45:2240–52.
[22] Nielsen P. Lecture notes on mixing ventilation. Technical report. Aalborg, Denmark: Department of Building Technology and Structural Engineering, Aalborg University; 1995.
[23] Nielsen P. Computational fluid dynamics and room air movement. Indoor Air 2004;14:134–43.
[24] Zhang T, Lee K, Chen Q. A simplified approach to describe complex diffusers in displacement ventilation for CFD simulations. Indoor Air 2009;19:255–67.
[25] Einberg G, Hagström K, Mustakallio P, Koskela H, Holmberg S. CFD modelling of an industrial air diffuser predicting the velocity and temperature in the near zone. Build Environ 2005;40:601–15.
[26] Weller H, Tabor G, Jasak H, Fureby C. A tensorial approach to computational continuum mechanics using object-oriented techniques. Comput Phys 1998;12:620–31.
[27] Mellin A. Tracer particles and seeding for particle image velocimetry. Meas Sci Technol 1997;8:1406–16.
[28] Toh I, Honnery D, Soria J. Axial plus tangential entry swirling jet. Exp Fluids 2010;48:309–25.
[29] Launder B, Sharma B. Application of the energy-dissipation model of turbulence to the calculation of the flow near a spinning disc. Lett Heat Mass Transfer 1974;1:131–8.
[30] Lemaire A. Air flow patterns within buildings. Subtask 1: room air and contaminat flow, evaluation of computational methods. Technical report. IEA Programme for Energy conservation in buildings and Comunity Systems; 1993.
[31] Koestel A. Paths of horizontally projected heated and chilled air jets. ASHRAE Trans 1955;61:213–32.
[32] Goodfellow H, Tahti E. Industrial ventilation design guidebook. Elsevier Academic Press; 2001.
[33] Lyakhovsky D, Syrkin S. Aerodynamics of the torch flowing out into the medium of another density. J Tech Phys 1939;9.
[34] Frean DH, Billington N. The ventilating air jets. J Institut Heat Vent Eng 1955;23:313–33.
[35] ASHRAE. Ashrae handbook: fundamentals. Atlanta: ASHRAE, Inc; 2009.